"Polysaccharide-based films for the prevention of unwanted postoperative adhesions at biological interfaces"

Sarah M. Mayes [a,*], Jessica Davis [a], Jessica Scott [a], Vanessa Aguilar [a], Scott A. Zawko [b], Steve Swinnea [b], Daniel L. Peterson [a], John G. Hardy [a,c*], Christine E. Schmidt [a,c*]

[a] Department of Biomedical Engineering, University of Texas at Austin, 107 W Dean Keeton St, Austin, TX 78712, USA; smayes78@gmail.com (S.M.); jedavi@ostatemail.okstate.edu (J.D.); jessica.scott@bcm.edu (J.S.); aguilsv@gmail.com (V.A.); johnhardyuk@gmail.com (J.G.H.); dlpeterson@me.com (D.L.P.)

[b] Department of Chemical Engineering, University of Texas at Austin, 200 E Dean Keeton St, Austin, TX 78712, USA; sazawko@gmail.com (S.A.Z.), swinnea@che.utexas.edu (S.S.).

[c] J. Crayton Pruitt Family Department of Biomedical Engineering, University of Florida, Biomedical Sciences Building JG-53, P.O. Box 116131, Gainesville, FL 32611-6131, USA; sazawko@gmail.com (S.A.Z.); schmidt@bme.ufl.edu (C.E.S.)

*denotes corresponding authors:

Sarah Mayes: smayes78@gmail.com; +1 (512) 739-9510 (tel); +1 (512) 549-2003 (fax); 6101 W. Courtyard Ln Ste 2-225, Austin, TX, 78730, USA.

John G. Hardy: johnhardyuk@gmail.com.

Christine Schmidt: schmidt@bme.ufl.edu; +1 (352) 273-9222 (tel); +1 (352) 273-9221 (fax); J. Crayton Pruitt Department of Biomedical Engineering, The University of Florida, Gainesville, FL, USA.

ABSTRACT.

Postoperative adhesions protect, repair, and supply nutrients to injured tissues; however, such adhesions often remain permanent and complicate otherwise successful surgeries by tethering tissues together that are normally separated. An ideal adhesion barrier should not only effectively prevent unwanted adhesions but should be easy to use, however, those that are currently available have inconsistent efficacy and are difficult to handle or to apply. A robust hydrogel film composed of alginate and a photo-crosslinkable hyaluronic acid (HA) derivative (glycidyl methacrylate functionalized hyaluronic acid (GMHA)) represents a solution to this problem. A sacrificial porogen (urea) was used in the film manufacture process to impart macropores that yield films that are more malleable and tougher than equivalent films produced without the sacrificial porogen. The robust mechanical behavior of these templated alginate/GMHA films directly facilitated handling characteristics of the barrier film. In a rat peritoneal abrasion model for adhesion formation, the polysaccharide films successfully prevented adhesions with statistical equivalence to the leading anti-adhesion technology on the market, Seprafilm®.

1. INTRODUCTION.

Postoperative adhesions are a major complication to otherwise successful surgeries [1-8]. Despite tremendous efforts to resolve this unwanted scar formation, there exists no consistently efficacious and safe solution [2, 4, 9, 10]. Adhesions form in the normal, acute phase of injury, and resolve in an equilibrium state between fibrin deposition and fibrinolysis until the injury site has healed [11-13]. However, these fibrinous strands may remain well beyond the healing period and tether tissues that are normally separated, causing chronic pain and even loss of function, such as secondary female infertility and bowel obstruction affecting the quality of life of the patients [2, 5, 10, 14-17]. Adhesion formation occurs in up to 90% of abdominopelvic procedures [8], requiring additional surgical interventions in over 33% of patients [18] which presents huge costs to the healthcare system (in excess of $3.45 billion (US) annually in the USA) [19-22].

Efforts to resolve unwanted adhesions have included improvements in surgical techniques [23], pharmaceutical methods [24], and barrier devices to mechanically separate tissues [3]. Mechanical devices have had the greatest success of any adhesion prevention method [13,25]. These devices include sprays, gels, solutions, *in situ* gelling polymers, and pre-formed membranes made from natural and synthetic polymers [10, 26].

A variety of adhesion prevention devices made from natural and synthetic polymeric materials have reached the Food and Drug Administration (FDA) approval. One of which is Seprafilm® (Sanofi, Paris, France), a pre-formed hydrogel membrane consisting of carboxymethylcellulose (CMC) and chemically modified HA. Despite its efficacy, the use of Seprafilm® is limited owing to its handling issues [27-29]. A dry Seprafilm is too brittle, sticks to tools, and is not repositionable; and the wet film has poor mechanical integrity and cannot be manipulated [2, 10]. Interceed® (Gynecare, Ethicon, Somerville, NJ) made from oxidized regenerated cellulose has

mixed reviews with some studies indicating adhesion induction [30] and limited efficacy in incomplete hemostasis [4]. Liquid based antiadhesion formulations like Adept™ (Baxter, Unterschleissheim, Germany) made of 4% icodextrin, is sutureless and can be administered laparoscopically, but its fluidity causes leakage from the surgical site with limited adherence to designated regions [31]. Some gels and *in situ* gelling formulations as adhesion barriers initially received much enthusiasm because of their ability to conform to tissue geometries and delivery via laparoscopy. However, injectable gels that are cross-linkable in situ were less favorable because of long gelling times and assistance required from external devices [2, 32-35]. The liquid based anti-adhesion agents are limited in their scope because they require complicated procedures to spray at the targeted site [31] and have failed due to dilution with bodily fluids and migration from the injury site [13], and crosslinked injectable gels such as Hyalobarrier® (Anika Therapeutics, S.r.l., Abano Terme, Italy) may be hindered by uneven distribution at the injury site [36].

An ideal anti-adhesion barrier should have the following attributes: be pliable, robust enough to withstand operating room procedures including laparoscopic delivery; maintain mechanical integrity to facilitate repositioning within the surgical field; conform to delicate tissue geometries; be mucoadhesive to avoid the need for sutures and staples; and have appropriate retention time to effectively prevent unwanted adhesions during the critical healing period of 3-7 days [37-39].

In this study, we present a pre-formed hydrogel membrane composed of HA and alginate, both are natural polysaccharides well established for wound healing and anti-adhesion [40-46]. The distinguishing feature of this membrane is a fibrillar ultrastructure attained by use of a sacrificial porogen (urea crystals) that imparts toughness and elasticity to the films. This ultrastructure is obtained by combining a photoreactive HA derivative, glycidyl methacrylate-hyaluronic acid (GMHA), alginate, and urea in aqueous solution. The solution is then cast into thin films, dried and nucleated with a urea seed crystal to initiate the growth of microscopic, branch-like urea crystals throughout the membrane. This *in situ* crystallization process compresses the polymers into microfibers [47], which are then stabilized by crosslinking with UV light and calcium chloride. Thoroughly rinsing the films with water washes away the urea crystals, leaving behind an interconnected porous network running alongside the fibers. This simple processing method does not require expensive equipment, software programming and is readily scalable. Furthermore, the resulting toughness and elasticity can be modified by tuning the membrane composition and crosslink density.

The alginate component in this membrane undergoes a gradual gel-to-mucoadhesive transition. Calcium ions responsible for gelation of the alginate are replaced with sodium ions, causing dissolution of the alginate into a mucous material [46]. This dissolution permits brief repositioning of the membranes in the surgical field, as well as subsequent mucous adherence to tissues.

The proposed innovative membrane solves the limitations of the existing anti-adhesion devices. This pre-formed membrane is easy to handle, can be manipulated while wet, is mucoadhesive, and can successfully prevent unwanted adhesions at a biological interface. Additionally, this membrane can be laparoscopically delivered, and requires no additional equipment or suturing. The unique fibrillar ultrastructure contributes to better mechanical and handling properties. In

addition, the porosity within the membrane facilitates the diffusion of water, nutrients and oxygen through the large surface area [48]. The form and mechanical characteristics of this adhesion barrier provide the foundation for excellent product efficacy.

2. MATERIALS AND METHODS.

2.1   Materials. Medical grade sodium alginate Pronova UP LVG: 120 kDa, M/G ratio 0.67 was purchased from FMC Novamatrix (Sandvika, Norway). High molecular weight sodium hyaluronate from *Streptococcus equi*. with molecular weight 1.6×10^6 Da was obtained from Sigma-Aldrich (St. Louis, MO, USA). Bacteria-derived high molecular weight sodium hyaluronate was also received from Genzyme, as a generous gift (1.6×10^6 MDa, Genzyme, Cambridge, MA, USA). Urea in the form of small round crystalline pellets was obtained from EM Science (Gibbs-town, NJ) and was used as provided. Photoinitiator Irgacure 2959 (I2959) was obtained from Ciba Specialty Chemicals (Basel, Switzerland). Photopolymerization was initiated by a long-wave UV chamber fitted with a mercury lamp filtered around 365 nm and with an intensity of 201 mWcm^{-2} (TOTAL-CURE UV Power Shot 1100 Curing Station, SPDI, Delray Beach, FL, USA). All other chemical reagents were obtained from Sigma-Aldrich. Dialysis tubing (3500 MWCO) was purchased from Spectrum Laboratories (Rancho Dominguez, CA, USA). Sterile filtration was conducted using 0.22 µm bottletop filters (Corning Life Sciences, Tewksbury, MA, USA).

2.2   Synthesis and Characterization of Glycidyl Methacrylate Functionalized Hyaluronic Acid (GMHA). Hyaluronic Acid (HA) was modified with photocrosslinkable methacrylate groups by adaptation of two protocols involving reaction of glycidyl methacrylate with hyaluronic acid (**Figure S1**) [47,49]. A 1% w/v solution of HA was prepared in a 50:50 mixture of acetone:water and stirred for 24 hours at room temperature. Twenty molar equivalents of each glycidyl methacrylate and triethylamine were added to the solution and stirred for 5 days at room temperature. GMHA was precipitated using a 20-fold volumetric excess of acetone and isolated by vacuum filtration. The GMHA precipitate was then dissolved in water for 24 hours at room temperature. The aqueous solution obtained was dialyzed against excess distilled, deionized (ddI) water for 72 hours and filter sterilized. The resulting solution was lyophilized and the GMHA was stored in the desiccators at -20 °C. GMHA obtained was dissolved in D$_2$O and characterized using solution state ^{1}H NMR spectroscopy (Varian INOVA 500 MHz). The ^{1}H NMR signals were referenced to the residual HOD signal, assigned a value of 4.78 ppm. A pre-saturation pulse was used to suppress the water peak. NMR data were processed with MestreLab MNOVA software. The degree of methacrylation (DM) was determined by integration of HA methyl protons (1.90 ppm) and methacrylate methyl protons (1.85 ppm), and was found to be 0.22 moles of methacryloyl groups per mole of disaccharide in HA (**Figure S2**) [10, 42, 43].

2.3   Preparation calcium alginate/GMHA films (non-templated). A 1% w/v solution of 67% alginate / 33% GMHA (11 or 32) (w/v) in ddI water was stirred at room temperature overnight with 0.05% photoinitiator. Solutions were cast in a 72 mm by 72 mm form. Forms were placed in a temperature and humidity controlled environmental chamber from Cincinnati Sub-Zero (Cincinnati, Oh). The temperature was held at 25 °C and humidity was held at 70% relative humidity (RH) during the casting period of 48 hours. Forms and solutions were kept from light at all times. Cast films were then subjected to UV light from the chamber, depending on the experiment. After photocrosslinking, if conducted, 50 mL of 100 mM calcium chloride

solution was pipetted on top of the cast film in the form. Films were left to crosslink for 30 minutes. Films were removed from molds, when possible, and transferred to petri dishes with large volumes of ddI water. Films were rinsed exhaustively in ddI water for 24 hours.

2.4   Preparation of alginate/GMHA films with sacrificial urea crystal template pores. A solution of 1% w/v of 67% alginate and 33% GMHA, 2% w/v of urea, and 0.05% w/v of Irgacure 2959 in ddI water was stirred at 25 ºC for 12 h, always protected from light using an aluminum foil around the container. Solutions were cast in custom-built polycarbonate forms (12.5 cm x 12.5 cm) and were placed in an environmental chamber (Cincinnati Sub-Zero, Cincinnati, OH, USA) maintained at 25 °C and 70% RH for 48 hours. Forms and solutions were protected from light at all times. At 48 hours, crystallization was initiated with urea seed crystals, as previously described by Zawko, et al [47]. The alginate/GMHA films were crosslinked by exposing to UV light for 30 s at a distance of 30 cm from the film surface. The films were then ionically crosslinked in 100 mM calcium chloride solution for 30 minutes followed by exhaustively rinsing with ddI water for 24 hours. Films prepared for in vitro and in vivo studies were maintained in sterile conditions in a laminar flow cabinet under UV light.

2.5   Thermogravimetric analysis (TGA). TGA testing (Mettler Toledo TGA 1 (Mettler-Toledo, Columbus, OH, USA) was used for the analysis of samples (ca. 1-4 mg) heated from 40°C to 400°C at a constant rate of 10 °C/min, under nitrogen gas pumped at 50 mL/min. All measurements were performed in triplicate (**Figure S3**).

2.6   Scanning Electron Microscopy (SEM). Films were air-dried for 24 hours, then sputter coated with 15 nm of platinum/palladium just prior to imaging on SEM (Zeiss Supra 40 VP) with an acceleration voltage of 10 kV.

2.7   Small Angle X-ray Scattering (SAXS). SAXS was conducted at the Texas Materials Institute. Data in the range (qlow) to (qhigh) were obtained from a Molecular Metrology custom SAXS instrument consisting of an Enraf-Nonious rotating copper anode source, double focusing beam conditioning (Ge mirror, Si(111) monochromator, Cu Kα radiation), and a 120 mm multiwire, gas filled proportional detector. Silver behenate was used as a calibration standard. 2D raw data were averaged to produce 1D data using Datasqueeze software (http://www.datasqueezesoftware.com).

2.8   Tensile testing of hydrogel films. Tensile testing was conducted according to ASTM standard method D882 [50] with minor modifications (detailed hereafter), on an Instron 3345 universal testing unit equipped with a BioPuls bath and pneumatic submergible smooth grips separated by a gauge length of 25.4 mm. A load of 100 N was applied at a constant cross head speed of 5 mm/min. Extension was measured with a video extensometer. Microsoft Excel software was used to process data. Film thicknesses were measured with a Vernier digital micrometer (BGS, Germany) having a measuring accuracy of 0.01 mm. The films obtained after cross-linking and rinsing were cut into strips 5 mm wide and 75 mm length. Thickness measurements were taken in triplicate for each strip. Films with variation in thickness greater than 10% were discarded in accordance with ASTM D882. Furthermore, any specimen with a thickness < 50 μm or >120 μm was also not included. Test samples were prepared with at least 24 hours of soaking in ddI water at 25 °C. Specimens were marked at the grips with a paint pen, for video extensometer recognition. An aqueous bath, at 25 °C, was lifted to submerge the

specimen, and tests were started immediately. Grip faces were wrapped in masking tape for tear prevention, as recommended by Instron. Specimens were pulled in tension at 5 mm/min strain rate until catastrophic failure. Proper test completion was considered to be any failure that did not occur at a nick, tear, or at other defect. The Young's modulus, measured in MPa, is a measure of intrinsic film stiffness [51], and was calculated according to the ASTM D882 (**Figure S4** for calculations) as the slope of the force–extension curve multiplied by the distance between the tension grips and divided by the original area of the specimen (length x thickness), (**Figure S4,** Equation 1). The elastic modulus (EM), tensile strength at break (TS), and percentage of elongation at break (%E) (**Figure S4,** Equation 2) were determined from the stress–Hencky strain curves, obtained from force–deformation data. Toughness (T, mJ) was determined as the area under the true stress-strain curve, until strain at break, ε_B (**Figure S4,** Equation 4). All measurements were performed in triplicate.

2.9   Dynamic mechanical analysis (DMA). Samples were prepared in the same way as that for tensile testing. Dynamic mechanical analysis was conducted on a TA Q800 with submergible chamber (TA Instruments, New Castle, DE). Films were pulled in tension for two testing sequences. The response to sinusoidal deformation over time was measured at 1 Hz frequency, 0.1% strain, and 15 mm specimen length for 2 hours. Frequency sweeps from 0.01 Hz to 200 Hz were conducted at 25 °C. The viscoelastic properties of the films were quantified in terms of the storage modulus (G'), the loss modulus (G''), and the mechanical loss factor tan δ. G' is a measure of the elastic or solid-like component, G'' is a measure of the viscous or liquid-like component, and tan δ = 1 gives the point of gelation. G' and G'' were recorded when steady-state was reached at a frequency of 1 Hz and represent the softness of the film, and the point of gelation gives an insight into the overall gel stability. All measurements were performed in triplicate.

2.10   Puncture testing of hydrogel films. Puncture tests were performed using an adaptation of ASTM D5748 (Protrusion Puncture Resistance of Stretch Wrap Films). A Texture Analyzer TA-XTplus (Stable Micro Systems, Godalming, UK) equipped with a 5 kg load cell and TexturePro CT software was used to analyze the films. The texture analyzer probe, TA39 with a probe head diameter of 2 mm and probe motion speed of 1 mm/sec was used for the puncture test. The force needed to puncture a square sample (25 × 25 mm) fixed in the TA-108S, the work done during this process, and the deformation of the film at the time of puncture were measured. Film thickness was measured using a screw micrometer (Mitutoyo, Neuss, Germany) and at five different places throughout the film.

2.11   Dissolution studies. After preparation and rinsing, films were cut with a six-inch blade into four equally sized pieces, with ribbing discarded. Film pieces were placed in a weighing boat in a dessication oven at 50 °C overnight. Dry weights were recorded using a high precision balance. Film pieces were exposed to 5, 10, 20, 30, 45, or 60 minutes in 100 mM citrate (pH 7.4) in dynamic conditions. At the determined time point, films were removed from citrate and washed three times in ddI water. Films were then dried in a dessication oven at 50 °C overnight. Final weights were recorded using a high precision balance. Throughout the dissolution study the films stayed in the same weigh boat except when being weighed. The dissolved film pieces did not stick to the weigh boat and could be easily removed without mechanical damage or loss of material.

2.12 In vitro cell culture studies

2.12.1 HDF cytocompatibility. Templated Alginate/GMHA-blended films used for cell studies were made under sterile conditions. Films were rinsed for 24 h and exhaustively washed with sterile water (WFI cell culture, Corning) prepared using 100 μL of gentamycin (50 μg/mL) in water. Cytotoxicity studies were conducted in accordance with ISO 10993-5 for in vitro cytotoxicity (ISO 2009). Briefly, 9.7 cm^2 of film was placed in 3 mL of cell culture medium (DMEM plus 10% FBS and 1:100 PSA) on a rocker at 37 °C for 24 hours. Human dermal fibroblasts (HDF, Cambrex) were seeded into 96-well tissue culture chambers at 15,000 cells/mL for 12 hours. Cells were then incubated with extractions from leaching media for 24 hours. Cells were fixed with 4% paraformaldehyde in phosphate-buffered saline (PBS, pH 7.4, 150 mM NaCl, 10 mM phosphate salts) and stained with 2 μM calcein AM and 4 μM ethidium homodimer-1 (Life Technologies, Grand Island NY, USA). Cell viability was assessed using the Celltiter Glo® luminescent cell viability assay (Promega, Madison WI, USA). All measurements were performed in triplicate.

2.12.2 HDF cell adhesion. To assess cell attachment to the templated Alginate/GMHA films, a direct-contact test was conducted in a custom-built polycarbonate well (2.54 cm x 2.54 cm x 3.81 cm) with a rubber gasket. The well was tightened over a templated film, or over a petri dish control surface. After assembly, poly-ι-lysine (PLL, 75-150 kDa, Sigma-Aldrich) was added to the wells over a petri dish control surface. After two hours, PLL was washed away by successive washes with PBS. Normal adult human dermal fibroblasts (HDF) cells were then seeded 20,000/well to all wells with 300 μL serum-free media (DMEM and 1:100 PSA). Samples were incubated for 3 hours at 37 °C, after which they were rinsed with PBS to remove non-adherent cells and fixed with 4% paraformaldehyde in PBS, and stained with 4´,6-diamidino-2-phenylindole (DAPI, 1:400 dilution in ddI water, Invitrogen) and phalloidin-Alexafluor 488 (1:300 dilution in blocking buffer, Invitrogen). Cells were imaged by epifluorescence at 20x magnification. All measurements were performed in triplicate.

2.13 In vivo studies

2.13.1 Rat cecal/sidewall abrasion model. All animal testing was conducted at The University of Texas at Austin Animal Research Center (UT-ARC) under the approval of the Institutional Animal Care and Use Committee (IACUC) for protocol AUP-2010-00164. Sprague-Dawley female rats aged 25-35 days (220 – 260 grams) were purchased from Charles River (Wilmington, MA), acclimated for 3 days, and maintained under a pathogen-free environment. All interventions were performed during the normal light or dark cycle. Animals were anesthetized with isoflurane (5% induction, 2% maintenance). A midline laparotomy incision of 4 cm was performed, and the cecum was identified. The entire surface of the cecum was abraded with sterile surgical gauze until the serosa was removed, as evidenced by redness and punctuate bleeding without hemostasis. Then, a defect of partial thickness in the abdominal wall was created by a #15 scalpel (Bard, Murray Hill, NJ, USA). Approximately 2 cm^2 of the parietal peritoneum was removed. Ten experimental rats received 9.7 cm^2 Seprafilm (Genzyme Corporation, Cambridge, MA) placed between the deserosalized surfaces. Ten animals received 9.7 cm^2 alginate/GMHA urea-templated films in the same manner. No additional interventions were performed to negative control animals (N=10) after the approximation of abraded cecum to the abraded abdominal wall. For all animals, the abdominal layers and skin incisions were closed

separately with interrupted 3.0 vicryl sutures on a SH needle (Ethicon, Somerville, NJ, USA), a nylon monofilament suture in a subcuticular fashion and surgical clips, when necessary. At 14 days postsurgery, the animals were sacrificed and the abdominal wall was exposed by a U-shaped incision to assess the presence and extent of adhesions. Adhesions were evaluated on a 4-point subjective scale by three clinical surgeons (Seton Family of Hospitals, TX, USA), who were blinded to the study specifics and results, and were otherwise not included in the surgical procedures. Adherence was evaluated post-mortem by gross observation, manual manipulation and irrigation with saline. Rats were monitored twice daily to ensure normothermia, satisfactory analgesia, and adequate respiratory function.

2.13.2 Adhesion grading scale. For each animal the number of adhesions and their anatomical locations were recorded. The severity of the adhesions was graded according to the tenacity or difficulty of separating the adhered tissues [18]. Grade 0 was assigned to animals that had no adhesions. Grade 1 was assigned to adhesions that were the least severe and separable by gravity alone. Grade 2 adhesions were moderately severe and were separable by blunt dissection. Grade 3 adhesions were the most severe, such as the whole of the cecum adhered directly to the abdominal wall, and were separable only by sharp dissection and unavoidable reinjury of the underlying tissue). Photographs of the different grades of adhesion can be found in the supporting information (**Figure S5**).

2.14 Statistical analysis. Kruskal-Wallis pairwise comparison was conducted on R software (Vienna University of Economics and Business, Austria). Statistical data are presented as mean ± standard deviation (SD). Student's t-test was used to compare mean values between the two groups (two-tailed). A difference of $p < 0.05$ was considered to be statistically significant.

3. RESULTS AND DISCUSSION

3.1 Film preparation. The successful modification of HA with glycidyl methacrylate (**Figure S1**) was confirmed by NMR (**Figure S2**). Optionally a simple method of imparting macropores within the films using urea crystals as sacrificial porogens (adapted from previously reported methodologies) [47] was employed, and TGA was used to confirm the removal of urea and other water soluble components (e.g. initiator and water soluble polymers not crosslinked to the films) from the films after extensive washing (**Figure S3**); urea is a metabolic product of protein digestion, generally regarded as safe by the FDA for a number of applications, and inexpensive, and therefore an interesting material to enable the production of macroporous biomaterials as tiny amounts of residue would not be expected to have a detrimental effect on the biological performance of the materials *in vivo*. The morphologies of the resultant films were studied by SEM (**Figure 1**), revealing the surface of non-templated films to be rough with pores not clustered (**Figure 1 A**), whereas the urea crystal templated films exhibited clustered pores with aligned microfibers of lengths/widths greater than 10 µm (**Figure 1 B and C**). These microfibers are also visible by naked eye (**Figure 1D**). Small angle X-ray scattering (SAXS) studies were used to observe changes in X-ray scattering intensity in the films (**Figure 2**). SAXS indicated a difference in scattering intensity at very low q ($Å^{-1}$) values that correspond to 5-130 nm. The scattering intensity below 5 nm looks similar for non-templated and urea templated films; however, for the larger scale features (130 nm), the scattering intensity was ca. 140% higher for the templated films at $q = 0.025$ $Å^{-1}$, which is associated with higher density of

features between 5-130 nm, suggesting a higher density of polymer chains in the urea templated films than the non-templated films, which will influence the mechanical properties.
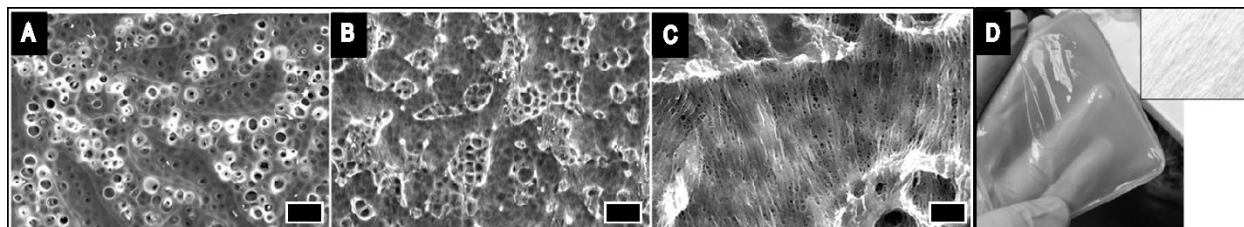

Figure 1. A-C) SEM images of Alginate/GMHA films. A) without crystal templating (scale bar 10μm). B) with urea crystal-templating (scale bar 10μm). C) with urea crystal-templating (scale bar 2μm). D) Photograph of Alginate/GMHA film prepared with urea templating with a contrast added close-up of film fibers in inset.
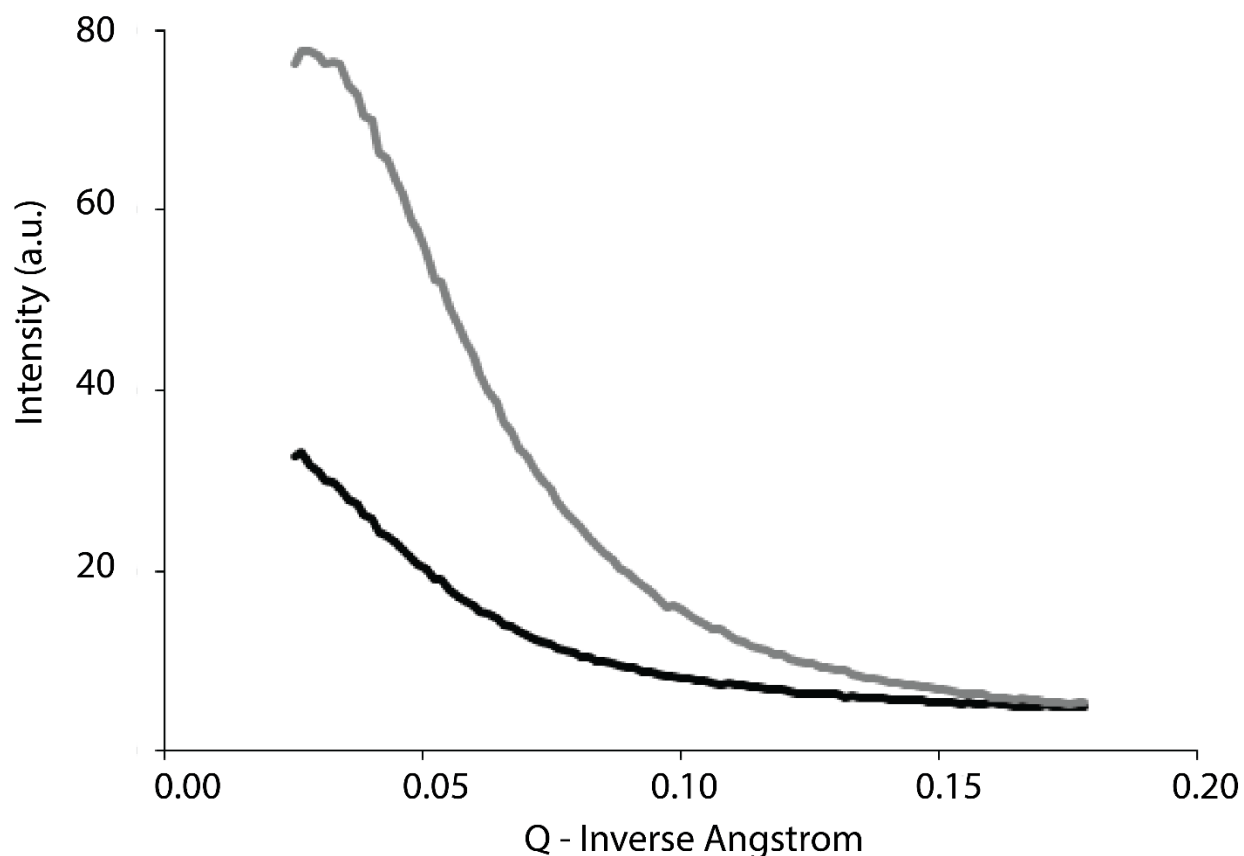

Figure 2. Small angle x-ray scattering (SAXS) of films. Black line) Alginate and GMHA films without urea crystal templating. Gray line) Alginate and GMHA films with urea crystal templating.

3.2   Mechanical properties of the films. The mechanical properties of medical devices are critical to their successful use [52-56]. Tensile testing is used extensively to determine the fundamental material properties (tensile strength, elongation at break, Young's modulus) of films [57-60], and dynamic mechanical analysis (DMA) testing is useful for understanding the

viscoelastic properties of films, where changes in storage and loss moduli are related to shifts in the solid-like and elastic-like components of a material, offering an insight into overall film stability. While these parameters are useful for the purposes of comparison, these tests are not specifically designed for testing films in a way that captures their handling properties: for instance, while tensile testing may provide toughness values, these values are highly sensitive to thickness measurements that may or may not be noticeable with regards to overall handleability, consequently we carried out puncture tests which are often used to capture handling properties of films (e.g. buccal films) [61]. The results of these mechanical tests on the films are summarized in **Table 1**.

Table 1. Mechanical Properties of alginate/GMHA non-templated films and alginate/GMHA urea templated films (based on calculations summarized in **Figure S4**).

	Non-templated films	Urea-templated films
Young's Modulus (MPa)	3.9 ± 1.1	3.3 ± 1.0
Tensile Strength (MPa)	3.8 ± 1.0	4.6 ± 0.6
Elongation (%)	97 ± 14	136 ± 22
Toughness (mJ)	9.7 ± 2.9	36.4 ± 14.1
Storage Modulus (MPa)	35.0 ± 4.7	22.1 ± 4.0
Loss Modulus (MPa)	4.2 ± 1.1	2.7 ± 1.5
Gelation point (Hz)	100 ± 3	N/A
Gelation point (Hz): Perpendicular to pores.	N/A	77 ± 3
Gelation point (Hz): Parallel to pores.	N/A	63 ± 4
% Elongation to break	67 ± 4	93 ± 10

The tensile strength of the films will be influenced by cross-linking of the alginate induced by calcium ions which results in gelation of the alginate component in the films, whereas the elongation is in part attributable to the macroporosity, water content and the ability of polymer chains to move (**Scheme S1**).

Urea templated films were pulled in tension and compared with non-templated films (**Table 1**). Urea templated films were pulled both parallel to and perpendicular to the visible pore direction, however, no statistically significant difference in values was found for large deformation testing, and therefore all urea templated films were combined and compared to non-templated films. Urea templated films had an insignificantly decreased Young's modulus when compared to non-templated films (p = 0.76); the modulus decreased (by 22%) which was within standard

deviation of the non-templated film; an increase in tensile strength (by 26%) of the templated films was not significantly different from the non-templated films ($p = 0.94$). The decrease in Young's modulus was a result of increased elongation (by 55%, which was not statistically significant ($p > 0.05$)). The toughness of a material is the amount of energy it stores prior to catastrophic failure, and it is ultimately a measure of allowed strain and is the area under the true stress-strain curve. As a result of markedly increased elongation, the toughness of templated films was as much as 500% higher than the non-templated films ($p < 0.05$).

Templating films via urea crystallization causes compression of viscous polymer around a crystalline network. The network of pores and fibers contribute to the mechanical properties of templated films. The polymer network in the fibers may be more dense than bulk polymers in non-templated films. Templating increases film toughness as a result of increased elongation. It is noteworthy that the macropores imparted by the sacrificial urea crystals and the basket-like fibrous mesh of dense polymer together facilitate greater elongation via compression of void volume and decompression of the polymers in templated films than in non-templated films when pulled in tension (**Scheme S1**, **Table 1**). The porous structure and the fibrous network in templated alginate/GMHA films allow greater stretch and strain (**Scheme S1**), and the higher density of polymer chains (as confirmed by SAXS measurements, **Figure 2**) offers a degree of reinforcement allowing greater elongation (or strain) to fail.

Dynamic mechanical analysis (DMA) provides a non-destructive mechanical analysis of materials by oscillating force within the linear elastic region, which was utilized to reveal the viscoelastic property changes imparted by urea templating. The storage and loss moduli were determined at 1 Hz (**Table 1**), the storage modulus (G') represents the solid-like component of a film, whereas the loss modulus (G") represents the liquid-like component of a film. Imparting pores to the films reduce both the G' and G" when compared to the non-templated films; G' significantly decreased (by 37%), and these values are in agreement with the tensile testing, suggesting an overall decrease in stiffness in the urea templated films. The anisotropic pores caused by urea crystallization in the templated films may be expected to impart anisotropic mechanical properties to the films [62]. High frequency sweeps were conducted to determine if the anisotropic pore direction could be detected in the urea templated films, where a material with a higher gelation point is considered more stable than a material with a lower gelation point. The gelation point is the abrupt change in viscosity of a solution arising from loss in fluidity and the formation of a 3-D network. The gelation point of the non-templated films was 100 ± 3 Hz, and that for the templated films was 76 ± 3 Hz when pulled perpendicular to the direction of the pores and 63 ± 3 Hz when pulled parallel to the direction of the pores. The urea templation process reduced the stability of an alginate/GMHA-blended film by approximately 21% and 35% when pulled perpendicular to and parallel to the direction of the pores, respectively. High frequency dynamic mechanical analysis indicated that templating decreased gel stability, with fiber alignment playing a role in that stability. These results confirm that there is fiber directionality which is not clearly demonstrated in large deformation testing. Thus, templated films are tougher, yet more liquid-like. Importantly, puncture tests revealed that templated films were significantly more pliable when compared to non-templated films (**Table 1**). The percent elongation to break for non-templated films was 67 ± 4, whereas for templated films was 93 ± 10 (a 38% increase relative to the non-templated films) which was also evident from the macroscopic handling perspective, as the templated films can withstand greater pulling and stretching.

3.3   In vitro validation studies. An in-vitro cytocompatibility study was conducted by culturing normal HDFs in the presence of degradation by-products of the templated alginate/GMHA films. HDFs were selected for this study as these cells are relevant to adhesion formation, and are responders to injury. The films were degraded in cell media consisting of DMEM plus 10% FBS and 1:100 PSA. A poly-L-lysine (PLL) coated tissue culture polystyrene control surface for optimal cell survival was compared to survival of cells exposed to 0.75% concentration of extract from the degraded film in media, per ISO 10993-5. Eight trials were run per film, and studies were conducted in triplicate including controls. Results were normalized per the PLL-coated tissue culture polystyrene control surface. Fibroblasts exposed to extracts of degraded films had the same cell survival rate at 24 h as that for fibroblasts on the PLL-coated substrates in the absence of the film byproducts ($p = 0.98$). This study established that the film degradation by-products are not cytotoxic (**Figure 3**) and supports further evaluation of these films for in-vivo studies.

The anti-adhesive behavior of templated alginate/GMHA blended films was assessed using HDFs in experimental conditions conducive for cellular adhesions. HDFs were selected for this study because they are known to adhere to a variety of surfaces via secretion of fibronectin which form prominent actin bundles [63]. Serum-free medium was used to prevent any serum interference with cellular adhesion. The attachment and proliferation of fibroblasts exposed on a PLL-coated plastic control surface and on the templated alginate/GMHA film surface in a serum-free medium was compared. Fibroblasts were assessed at six hours after seeding, and imaged by epifluorescence at 20x magnification. While positive control PLL-coated plastic substrates supported the attachment of HDFs, as shown with DAPI and phalloidin stained HDFs (**Figure 3**), HDF attachment on the surfaces of the polysaccharide films was vastly reduced (by 96.79% $\pm$ 3.37%) when compared to the PLL-coated plastic, confirming that the polysaccharide films are non-adhesive. Alginate and HA containing films are highly hydrophilic and have anti-adhesion properties in part because of their anionic nature [46,64].
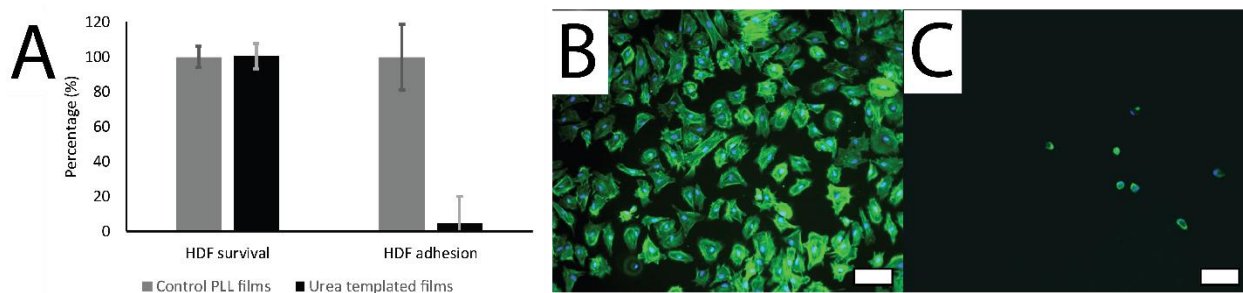

Figure 3. In vitro assessment of Human Dermal Fibroblast attachment and survival on films. **A)** Cytocompatibility: HDF survival (%) when exposed to degraded urea templated alginate/GMHA film effluent (0.75% concentration of extract from degraded film in media, per ISO 10933-5) normalized relative to a PLL control surface (time = 24 hours, experimental number = 24). HDF adhesion (%) in serum-free medium normalized relative to a PLL control surface. **B)** HDFs on PLL. **C)** HDFs on non-templated Alginate/GMHA films. HDFs were stained with DAPI and phalloidin. Scale bars represent 100 μm.

For success as an anti-adhesion barrier, the dissolution rate should be high. To understand the impact that templating had on dissolution we exposed templated and non-templated films to 0.1

M citrate to chelate the calcium ions (**Figure S5**). Dissolution begins upon release of calcium ions and the GMHA remnants are not visible in aqueous solutions. Templating reduced the dissolution rate of films (concomitant with increased chain density **Figure 2**), extending the theoretical in vivo residence time. At 60 minutes, the mass of template films remaining was $25.6\% \pm 3.6$ of the mass at the start, and completely dissolved after 120 minutes; by contrast the non-templated films dissolved within 30 minutes. The observed film dissolution upon calcium ion release facilitates brief repositioning of the membranes in the surgical field, as well as subsequent mucous adherence to tissues.

3.4 In vivo validation studies. The in-vitro cytocompatibility and fibroblast adhesion study provided efficacious data to support the application of alginate/GMHA films for prevention of post-operative adhesions. In vivo validation tests used a rat peritoneal (cecal/sidewall) abrasion model (**Figure 4**) which is defined, documented, and accepted as the optimal model for anti-adhesion testing [65-68]. Rat abdominal adhesions form quickly, can be assessed grossly on an industry-accepted subjective scale (**Figure 5, Figure S6** and **Figure S7**), and are most similar to human adhesion formation in both timing and placement [69]. While there are slight variations of this model, the general approach involves placing two injured tissue surfaces in proximity to each other, either without or with a barrier between them, followed by assessment of adhesion formation between the two injured surfaces. A pilot efficacy study was conducted with 30 animals (3 groups, N=10): one group of 10 rats was a negative control group that received no treatment; one group of 10 rats was a positive control group that received the leading commercially available anti-adhesion device, Seprafilm®; and the experimental group received urea templated alginate/GMHA films. Necropsy was conducted at 14 days post operation and the results are summarized in **Table 2**. There were no signs of hemorrhage, infection or unexpected death of animals before the planned sacrifice time.
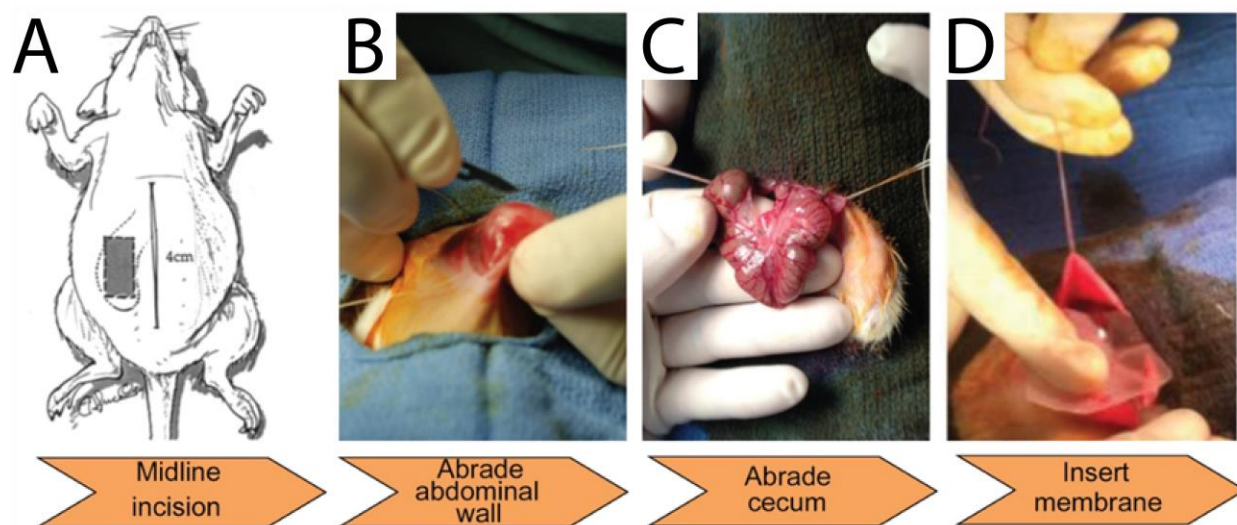

Figure 4. Rat cecal/sidewall abrasion model of abdominal adhesions. A) The rat abdominal cavity was opened by midline incision. B) 6.5 cm^2 section of the abdomen was abraded with a scalpel. C) The entire surface of the cecum was abraded with sterile gauze. D) Insertion of membrane for anti-adhesion efficacy testing between the cecum and abdominal wall.
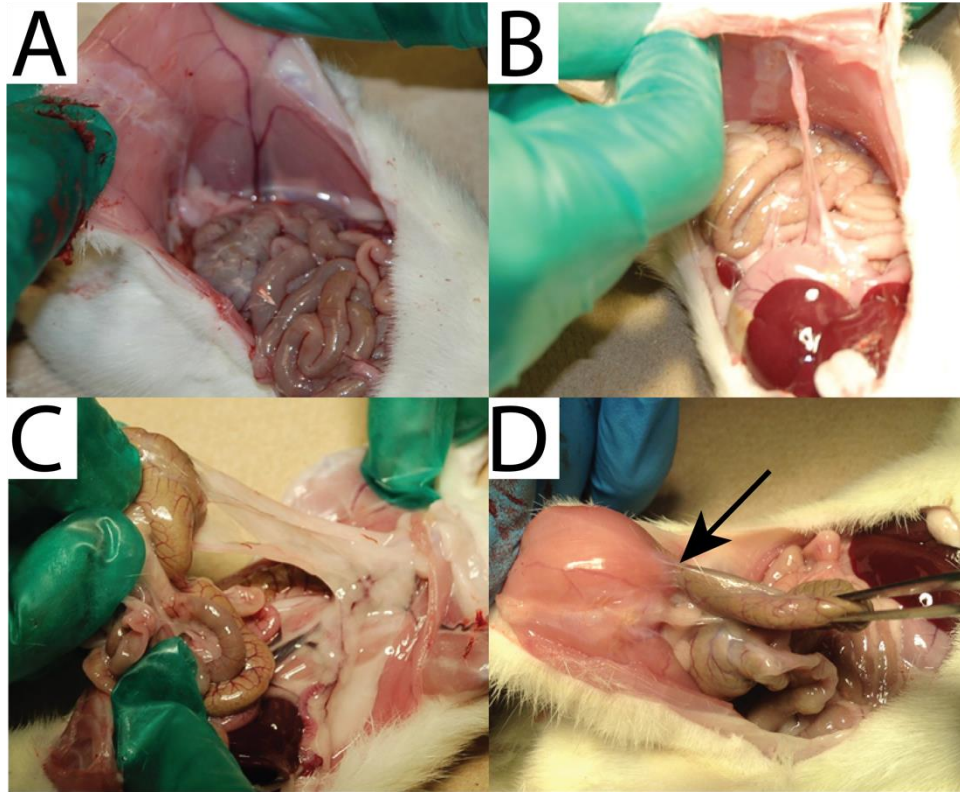
Figure 5. Adhesion grading scale. A) Grade 0: no adhesions. B) Grade 1: Least severe adhesions, separable by gravity. C) Grade 2: moderate severity adhesions, separable by blunt dissection. D) Grade 3: Severe adhesions, separable only by sharp dissection. Arrow indicates a fibrous adhesion tethering the cecum to the abdominal wall.

Table 2. Results of in vivo studies

	Grade 0	**Grade 1**	**Grade 2**	**Grade 3**	**p-value**	**Film Remnant**
Control	1	0	2	7	N/A	N/A
Seprafilm®	8	0	1	1	0.0020	0
Urea-templated film	9	0	1	0	0.0004	7

Cecum-to-abdominal wall adhesions were successfully induced using the sidewall defect and cecum abrasion model in rats. Adhesions in 90% of untreated negative control animals (animals that were injured but received no barrier agent treatment on the defect) indicated successful implementation of this animal model. These were heavy adhesions around the peritoneum and cecum, and sharp dissection was required to detach the large fibrous tissue bridging the surroundings of both. The positive control, Seprafilm® treatment, successfully prevented unwanted adhesions in 80% of the animals. This value is statistically significant when compared to the negative control group (p = 0.002). The remaining 20% of animals treated with

Seprafilm® suffered with heavy adhesions with scores 2 and 3. The urea templated alginate/GMHA films successfully prevented adhesions in 90% of the animals. This value is statistically significant when compared to the negative control group ($p = 0.004$). The defects were almost repaired within two weeks. Only 1 out of 10 animals showed moderately severe adhesions that was separable by a blunt dissection. Both treatment groups prevented adhesions with statistical significance compared to the untreated controls ($p < 0.05$). Effective membranes are anticipated to exhibit grade 0 adhesions in greater than 70% of the treated animals based on literature reports for HA/CMC membranes in the rat cecal abrasion model (Burns *et al* 1997). The results of this pilot study demonstrate that the templated alginate/HA films are effective at preventing adhesions without impacting the normal tissue healing process.

This study demonstrated that the templated alginate/GMHA films possess favorable handling properties and can be successfully used as anti-adhesion barriers. The alginate/GMHA films are mechanically robust, can be rolled up for laparoscopic insertion, can be applied wet, and are briefly repositionable, which represents an advantage over the current market leader Seprafilm®. Furthermore, presence of film in vivo at 14 days postoperative suggests a longer dissolution rate than Seprafilm®. This reduced dissolution rate could be exploited for an indication with longer-term residence or combined with semi-prolonged drug release.

4.0 CONCLUSIONS

Here we present polysaccharide membranes with anti-adhesive properties that address a specific clinical need for materials that are easy to handle and deter/prevent postoperative adhesions between biological interfaces. A simple, bench-top process using urea as a sacrificial porogen enabled the creation of macropores within three-dimensional alginate/GMHA films. The resulting films that are more malleable and tougher than equivalent films produced without the sacrificial porogen. In a rat peritoneal abrasion model for adhesion formation, the polysaccharide films successfully prevented adhesions with statistical equivalence to the leading anti-adhesion technology on the market, Seprafilm®.

REFERENCES

[1] M.A. Weibel, G. Majno, Peritoneal adhesions and their relation to abdominal surgery. A postmortem study, Am J Surg 126 (1973) 345-353.

[2] C.H. Lee, H. Kim, I.W. Han, S.M. Kim, B.S. Kwak, Y.H. Baik, Y.J. Park, M.G. Oh, Effect of polylactic film (Surgi-Wrap) on preventing postoperative ileus after major hepato-pancreato-biliary surgery, Ann Hepatobiliary Pancreat Surg 20(4) (2016) 191-196.

[3] P. Mattei, J.L. Rombeau, Review of the pathophysiology and management of postoperative ileus, World J Surg 30 (2006) 1382-1391.

[4] A. Hirschelmann, G. Tchartchian, M. Wallwiener, A. Hackethal, R.L. De Wilde, A review of the problematic adhesion prophylaxis in gynaecological surgery, Arch Gynecol Obstet 285(4) (2012) 1089-97.

[5] D. Menzies, H. Ellis, Intestinal obstruction from adhesions--how big is the problem?, Ann R Coll Surg Engl 72 (1990) 60-63.

[6] M.L. Harris, The use of silver foil to prevent adhesions in brain surgery, JAMA 42 (1904) 763-765.

[7] H. Ellis, Cause and prevention of postoperative intraperitoneal adhesions, Surgery Gynecology and Obstetrics with International Abstracts of Surgery 133(3) (1971) 497-511.

[8] H. Ellis, B.J. Moran, J.N. Thompson, M.C. Parker, M.S. Wilson, D. Menzies, A. McGuire, A.M. Lower, R.J. Hawthorn, F. O'Brien, S. Buchan, A.M. Crowe, Adhesion-related hospital readmissions after abdominal and pelvic surgery: a retrospective cohort study, Lancet 353(9163) (1999) 1476-80.

[9] C. Brochhausen, V.H. Schmitt, T.K. Rajab, C.N.E. Planck, B. Krämer, M. Wallwiener, H. Hierlemann, C.J. Kirkpatrick, Intraperitoneal adhesions—An ongoing challenge between biomedical engineering and the life sciences, J. of Biomed. Mater. Res. 98A(1) (2011) 143-156.

[10] J. Li, X. Feng, B. Liu, Y. Yu, L. Sun, T. Liu, Y. Wang, J. Ding, X. Chen, Polymer materials for prevention of postoperative adhesion, Acta Biomater 61 (2017) 21-40.

[11] J.B. Van der Wal, J. Jeekel, Biology of the peritoneum in normal homeostasis and after surgical trauma, Colorectal Dis. 9 (2007) 9-13.

[12] H. Sulaiman, G. Gabella, C. Davis MSc, S.E. Mutsaers, P. Boulos, G.J. Laurent, S.E. Herrick, Presence and distribution of sensory nerve fibers in human peritoneal adhesions, Ann. Surg. 234(2) (2001) 256-261.

[13] B.C. Ward, A. Panitch, Abdominal Adhesions: Current and Novel Therapies, J. Surg. Res. 165(1) (2011) 91-111.

[14] M. Ouaïssi, S. Gaujoux, N. Veyrie, E. Denève, C. Brigand, B. Castel, J.J. Duron, A. Rault, K. Slim, D. Nocca, Post-operative adhesions after digestive surgery: their incidence and prevention: review of the literature, J. Visc. Surg. 149(2) (2012) 104-114.

[15] H. Van Goor, Consequences and complications of peritoneal adhesions, Colorectal Dis. 9 (2007) 25-34.

[16] G.S. diZerega, Contemporary adhesion prevention, Fertil. Steril. 61(2) (1994) 219-235.

[17] Y.J.Z. Ren, Z. Y.; Cui, F.; Wang, Y.; Zhao, J.; Xu, Q., Hyaluronic acid/polylysine hydrogel as a transfer system for transplantation of neural stem cells., J. Bioact. Comp. Polym. 24 (2009) 56-62.

[18] Y. Yeo, C.B. Highley, E. Bellas, T. Ito, R. Marini, R. Langer, D.S. Kohane, In situ cross-linkable hyaluronic acid hydrogels prevent post-operative abdominal adhesions in a rabbit model, Biomaterials 27(27) (2006) 4698-4705.

[19] D.M. Wiseman, R. Meidler, Y. Lyahovetsky, E. Kurman, S. Horn, I. Nur, Evaluation of a fibrin preparation containing tranexamic acid (Adhexil) in a rabbit uterine horn model of adhesions with and without bleeding and in a model with two surgical loci, Fertil. Steril. 93(4) (2010) 1045-1051.

[20] C.Z. Beck D. E, Fleshman J. W, Kaufman H. S., van Goor H., Wolff B. G., A prospective, randomized, multicenter, controlled study of the safety of Seprafilm adhesion barrier in abdominopelvic surgery of the intestine Dis Colon Rectum 46 (2003) 1310-1319.

[21] Q. Zeng, Z. Yu, J. You, Q. Zhang, Efficacy and safety of Seprafilm for preventing postoperative abdominal adhesion: systematic review and meta-analysis, World J Surg 31 (2007) 2125-2131.

[22] C. Brochhausen, V.H. Schmitt, C.N. Planck, T.K. Rajab, D. Hollemann, C. Tapprich, B. Krämer, C. Wallwiener, H. Hierlemann, R. Zehbe, H. Planck, C.J. Kirkpatrick, Current strategies and future perspectives for intraperitoneal adhesion prevention, J. Gastrointest. Surg. 16(6) (2012) 1256-1274.

[23] L. Holmdahl, B. Risberg, D.E. Beck, J.W. Burns, N. Chegini, G.S. diZerega, H. Ellis, Adhesions: pathogenesis and prevention-panel discussion and summary, Eur. J. Surg. Suppl. 577 (1997) 56-62.

[24] Y. Liu, H. Li, X.Z. Shu, S.D. Gray, G.D. Prestwich, Crosslinked hyaluronan hydrogels containing mitomycin C reduce postoperative abdominal adhesions, Fertil. Steril. 83 Suppl 1 (2005) 1275-83.

[25] L.A. Gago, G.M. Saed, S. Chauhan, E.F. Elhammady, M.P. Diamond, Seprafilm (modified hyaluronic acid and carboxymethylcellulose) acts as a physical barrier, Fertil. Steril. 80(3) (2003) 612-616.

[26] J. Zhang, H. Liu, H. Xu, J.-X. Ding, X.-L. Zhuang, X.-S. Chen, F. Chang, J.-Z. Xu, Z.-M. Li, Molecular weight-modulated electrospun poly(ε-caprolactone) membranes for postoperative adhesion prevention, RSC Advances 4(79) (2014) 41696-41704.

[27] I. Kusuki, I. Suganuma, F. Ito, M. Akiyama, A. Sasaki, K. Yamanaka, H. Tatsumi, J. Kitawaki, Usefulness of Moistening Seprafilm Before Use in Laparoscopic Surgery, Surg Laparosc Endosc Percutan Tech. 24(1) (2014) e13-e15.

[28] M.K. Hong, D.-C. Ding, Seprafilm® Application Method in Laparoscopic Surgery, JSLS, 2017, p. e2016.00097.

[29] L. Allegre, I. Le Teuff, S. Leprince, S. Warembourg, H. Taillades, X. Garric, V. Letouzey, S. Huberlant, A new bioabsorbable polymer film to prevent peritoneal adhesions validated in a post-surgical animal model, PLoS One 13(11) (2018) e0202285.

[30] H.A. Kayaoglu, N. Ozkan, S.M. Hazinedaroglu, O.F. Ersoy, R.D. Koseoglu, An Assessment of the Effects of Two Types of Bioresorbable Barriers to Prevent Postoperative Intra-Abdominal Adhesions in Rats, Surg. Today 35(11) (2005) 946-950.

[31] C.H. Chen, S.H. Chen, S.H. Mao, M.J. Tsai, P.Y. Chou, C.H. Liao, J.P. Chen, Injectable thermosensitive hydrogel containing hyaluronic acid and chitosan as a barrier for prevention of postoperative peritoneal adhesion, Carbohydr Polym 173 (2017) 721-731.

[32] Y. Yeo, C.B. Highley, E. Bellas, T. Ito, R. Marini, R. Langer, D.S. Kohane, In situ cross-linkable hyaluronic acid hydrogels prevent post-operative abdominal adhesions in a rabbit model, Biomaterials 27(27) (2006) 4698-705.

[33] Y. Yeo, M. Adil, E. Bellas, A. Astashkina, N. Chaudhary, D.S. Kohane, Prevention of peritoneal adhesions with an in situ cross-linkable hyaluronan hydrogel delivering budesonide, J. Control. Release 120(3) (2007) 178-85.

[34] J.A. Burdick, G.D. Prestwich, Hyaluronic acid hydrogels for biomedical applications, Advanced materials (Deerfield Beach, Fla.) 23(12) (2011) H41-H56.

[35] M.-W. Lee, H.-F. Tsai, S.-M. Wen, C.-H. Huang, Photocrosslinkable gellan gum film as an anti-adhesion barrier, Carbohydrate Polymers 90(2) (2012) 1132-1138.

[36] E. Yurdakul Sikar, H.E. Sikar, H. Top, A.C. Aygit, Effects of Hyalobarrier gel and Seprafilm in preventing peritendinous adhesions following crush-type injury in a rat model, Ulus. Travma Acil Cerrahi Derg. 25(2) (2019) 93-98.

[37] S.Y. Na, S.H. Oh, K.S. Song, J.H. Lee, Hyaluronic acid/mildly crosslinked alginate hydrogel as an injectable tissue adhesion barrier, J. Mater. Sci. Mater. Med. 23 (2012) 2303-2313.

[38] N.W. Q. Wu, T. He, J. Shang, L. Li, L. Song, X. Yang, X. Li, N. Luo, W. Zhang, C. Gong, , p. 13553, Thermosensitive hydrogel containing dexamethasone micelles for preventing postsurgical adhesion in a repeated-injury model, Sci. Rep. 5 (2015) 13553.

[39] Y.L.W. K. Shi, Y. Qu, J.F. Liao, B.Y. Chu, H.P. Zhang, F. Luo, Z.Y. Qian, Synthesis, characterization, and application of reversible PDLLA-PEG-PDLLA copolymer thermogels in vitro and in vivo, Sci. Rep. 6 (2016) 19077.

[40] G. Blaine, Experimental Observations on Absorbable Alginate Products in Surgery * Gel, Film, Gauze and Foam, Ann Surg 125(1) (1947) 102-114.

[41] S.M. Kuo, Chang, S.J., Wang, H. Y., Tang, S. C. & Yang, S. W. , Evaluation of the ability of xanthan hum/gellan gum/hyaluronan hydrogel membranes to prevent the adhesion of postrepaired tendons., Carbohydrate Polymers 114 (2014) 230-237.

[42] C.H.C. S.H. Chen, K.T. Shalumon, J.P. Chen, Preparation and characterization of antiadhesion barrier film from hyaluronic acid-grafted electrospun poly(caprolactone) nanofibrous membranes for prevention of flexor tendon postoperative peritendinous adhesion, Int. J. Nanomed. 9 (2014) 4079-4092.

[43] L. Li, N. Wang, X. Jin, R. Deng, S. Nie, L. Sun, Q. Wu, Y. Wei, C. Gong, Biodegradable and injectable in situ cross-linking chitosan-hyaluronic acid based hydrogels for postoperative adhesion prevention, Biomaterials 35 (2014) 3903-3917.

[44] M. Davidovich-Pinhas, H. Bianco-Peled, Alginate-PEGAc: a new mucoadhesive polymer, Acta Biomater 7(2) (2011) 625-33.

[45] C.E. Schanté, G. Zuber, C. Herlin, T.F. Vandamme, Chemical modifications of hyaluronic acid for the synthesis of derivatives for a broad range of biomedical applications, Carbohydrate Polymers 85(3) (2011) 469-489.

[46] W.J. Cho, S.H. Oh, J.H. Lee, Alginate Film as a Novel Post-Surgical Tissue Adhesion Barrier, J. Biomater. Sci. Polym. Ed. 21(6-7) (2010) 701-713.

[47] S.A. Zawko, C.E. Schmidt, Crystal templating dendritic pore networks and fibrillar microstructure into hydrogels, Acta Biomater 6(7) (2010) 2415-21.

[48] J.H. Kim, S.B. Lee, S.J. Kim, Y.M. Lee, Rapid temperature/pH response of porous alginate-g-poly(N-isopropylacrylamide) hydrogels, Polymer Communication 43 (2002) 7549-7558.

[49] S.A. Bencherif, A. Srinivasan, F. Horkay, J.O. Hollinger, K. Matyjaszewski, N.R. Washburn, Influence of the degree of methacrylation on hyaluronic acid hydrogels properties, Biomaterials 29(12) (2008) 1739-49.

[50] ASTM, Annual Book of ASTM Standards, Standard test method for tensile properties of thin plastic sheeting. Standard designations: D882.

[51] N. Cao, Y. Fu, J. He, Mechanical properties of gelatin films cross-linked, respectively, by ferulic acid and tannin acid, Food Hydrocolloids 21(4) (2007) 575-584.

[52] Multilayer Thin Films, Wiley-VCH Verlag GmbH & Co. KGaA2002.

[53] K. Peh, T. Khan, H. Ch'ng, Mechanical, bioadhesive strength and biological evaluations of chitosan films for wound dressing, J. Pharm. Pharm. Sci. 3(3) (2000) 303-311.

[54] G.S. Macleod, J.T. Fell, J.H. Collett, Studies on the physical properties of mixed pectin/ethylcellulose films intended for colonic drug delivery, Int. J. Pharm. 157(1) (1997) 53-60.

[55] M.S. Nagarsenker, D.D. Hegde, Optimization of the mechanical properties and water-vapor transmission properties of free films of hydroxypropylmethylcellulose, Drug Dev. Ind. Pharm. 25(1) (1999) 95-8.

[56] A.D. Sezer, F. Hatipoglu, E. Cevher, Z. Ogurtan, A.L. Bas, J. Akbuga, Chitosan film containing fucoidan as a wound dressing for dermal burn healing: preparation and in vitro/in vivo evaluation, AAPS PharmSciTech 8(2) (2007) E94-E101.

[57] S.M. Pawde, K. Deshmukh, Characterization of polyvinyl alcohol/gelatin blend hydrogel films for biomedical applications, J. Appl. Polym. Sci. 109(5) (2008) 3431-3437.

[58] T. Fujie, N. Matsutani, M. Kinoshita, Y. Okamura, A. Saito, S. Takeoka, Adhesive, Flexible, and Robust Polysaccharide Nanosheets Integrated for Tissue-Defect Repair, Adv. Funct. Mater. 19(16) (2009) 2560-2568.

[59] M.A. García, A. Pinotti, M. Martino, N. Zaritzky, Electrically treated composite FILMS based on chitosan and methylcellulose blends, Food Hydrocolloids 23(3) (2009) 722-728.

[60] F. Febriyenti, A. Noor, S. Bin Bai, Mechanical properties and water vapour permeability of film from Haruan (Channa striatus) and Fusidic acid spray for wound dressing and wound healing, Pak. J. Pharm. Sci. 23 (2010) 155-9.

[61] M. Preis, C. Woertz, K. Schneider, J. Kukawka, J. Broscheit, N. Roewer, J. Breitkreutz, Design and evaluation of bilayered buccal film preparations for local administration of lidocaine hydrochloride, Eur. J. Pharm. Biopharm. 86(3) (2014) 552-61.

[62] R. Kasada, S.G. Lee, J. Isselin, J.H. Lee, T. Omura, A. Kimura, T. Okuda, M. Inoue, S. Ukai, S. Ohnuki, T. Fujisawa, F. Abe, Anisotropy in tensile and ductile–brittle transition behavior of ODS ferritic steels, J. Nucl. Mater. 417(1) (2011) 180-184.

[63] K. Nishimura, P. Blume, S. Ohgi, B.E. Sumpio, Effect of different frequencies of tensile strain on human dermal fibroblast proliferation and survival, Wound Repair Regen. 15(5) (2007) 646-656.

[64] I.F. Sufiyarov, Experimental validation for the use of a film on the basis of modified hyaluronic acid for prevention of postoperative peritoneal adhesions, Bull. Exp. Biol. Med. 144(2) (2007) 269-71.

[65] E. Ersoy, V. Ozturk, A. Yazgan, M. Ozdogan, H. Gundogdu, Comparison of the two types of bioresorbable barriers to prevent intra-abdominal adhesions in rats, J. Gastrointest. Surg. 13(2) (2009) 282-6.

[66] H.Y. Lo, H.T. Kuo, Y.Y. Huang, Application of polycaprolactone as an anti-adhesion biomaterial film, Artif. Organs 34(8) (2010) 648-53.

[67] T.K. Rajab, M. Wallwiener, C. Planck, C. Brochhausen, B. Kraemer, C.W. Wallwiener, A direct comparison of seprafilm, adept, intercoat, and spraygel for adhesion prophylaxis, J. Surg. Res. 161(2) (2010) 246-9.

[68] T.-D. Way, S.-R. Hsieh, C.-J. Chang, T.-W. Hung, C.-H. Chiu, Preparation and characterization of branched polymers as postoperative anti-adhesion barriers, Appl. Surf. Sci. 256(10) (2010) 3330-3336.

[69] H. Ozel, F.M. Avsar, S. Topaloglu, M. Sahin, Induction and assessment methods used in experimental adhesion studies, Wound Repair Regen. 13(4) (2005) 358-364.

Supplementary Information
Polysaccharide-based films for the prevention of unwanted postoperative adhesions at biological interfaces

Sarah M. Mayes [a,*], Jessica Davis [a], Jessica Scott [a], Vanessa Aguilar [a], Scott A. Zawko [b], Steve Swinnea [b], Daniel L. Peterson [a], John G. Hardy [a,c*], Christine E. Schmidt [a,c*]

[a] Department of Biomedical Engineering, University of Texas at Austin, 107 W Dean Keeton St, Austin, TX 78712, USA.

[b] Department of Chemical Engineering, University of Texas at Austin, 200 E Dean Keeton St, Austin, TX 78712, USA.

[c] J. Crayton Pruitt Family Department of Biomedical Engineering, University of Florida, Biomedical Sciences Building JG-53, P.O. Box 116131, Gainesville, FL 32611-6131, USA.

Hyaluronic acid (HA)

Glycidyl methacrylate functionalized hyaluronic acid (GMHA)
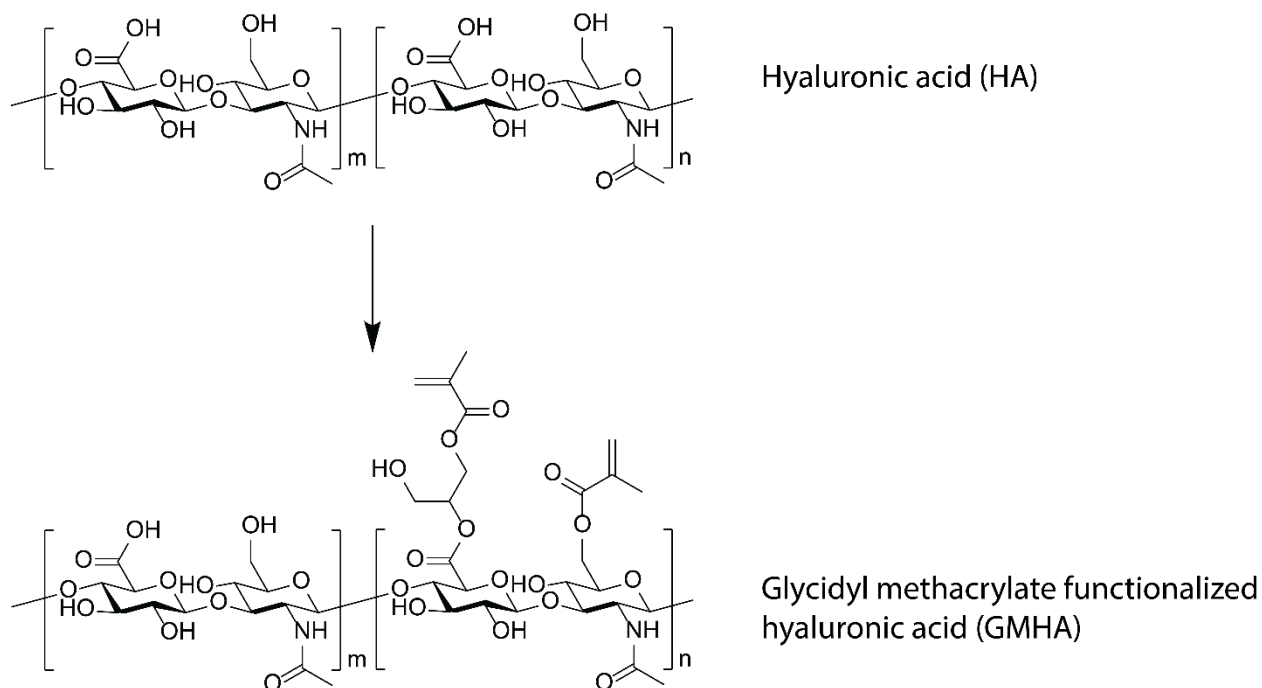
Figure S1. Conversion of hyaluronic acid to glycidyl methacrylate functionalized hyaluronic acid.
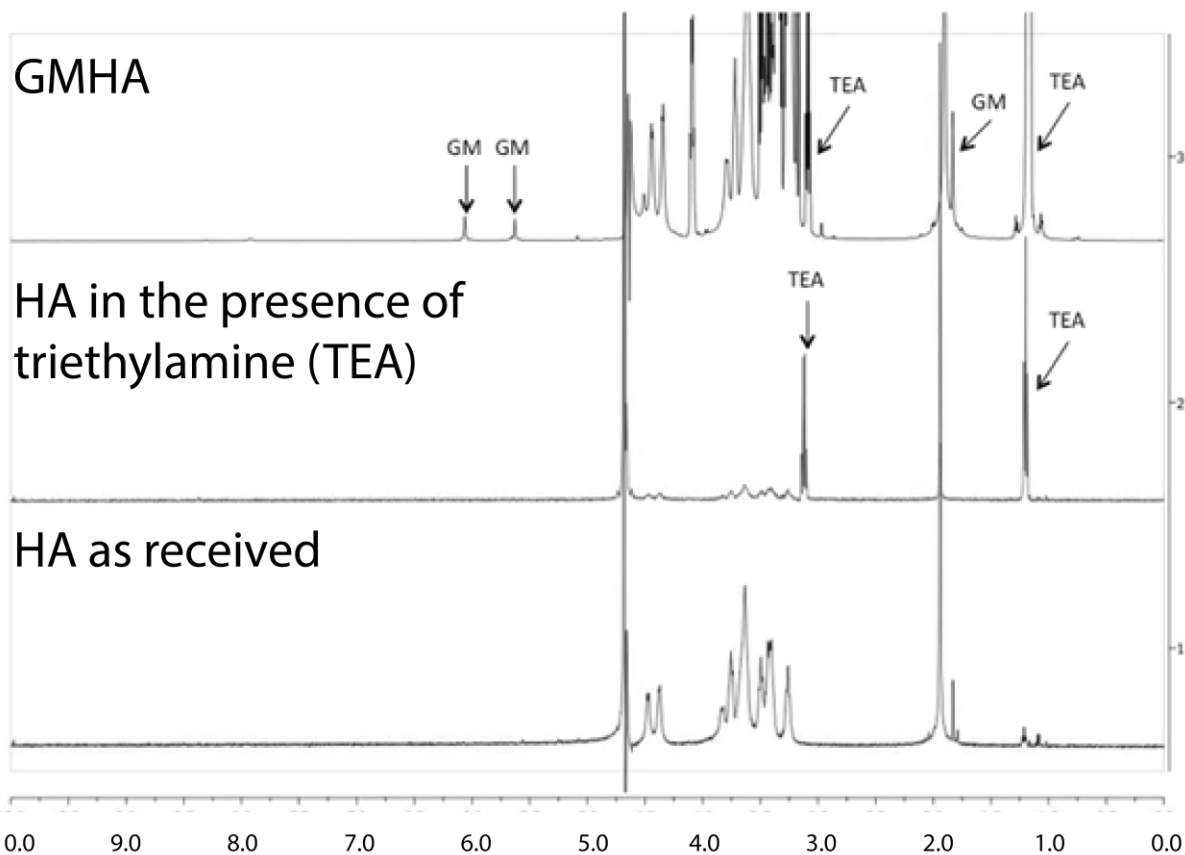
Figure S2. NMR spectra of hyaluronic acid alone, in the presence of trimethylamine and modified with glycidyl methacrylate.
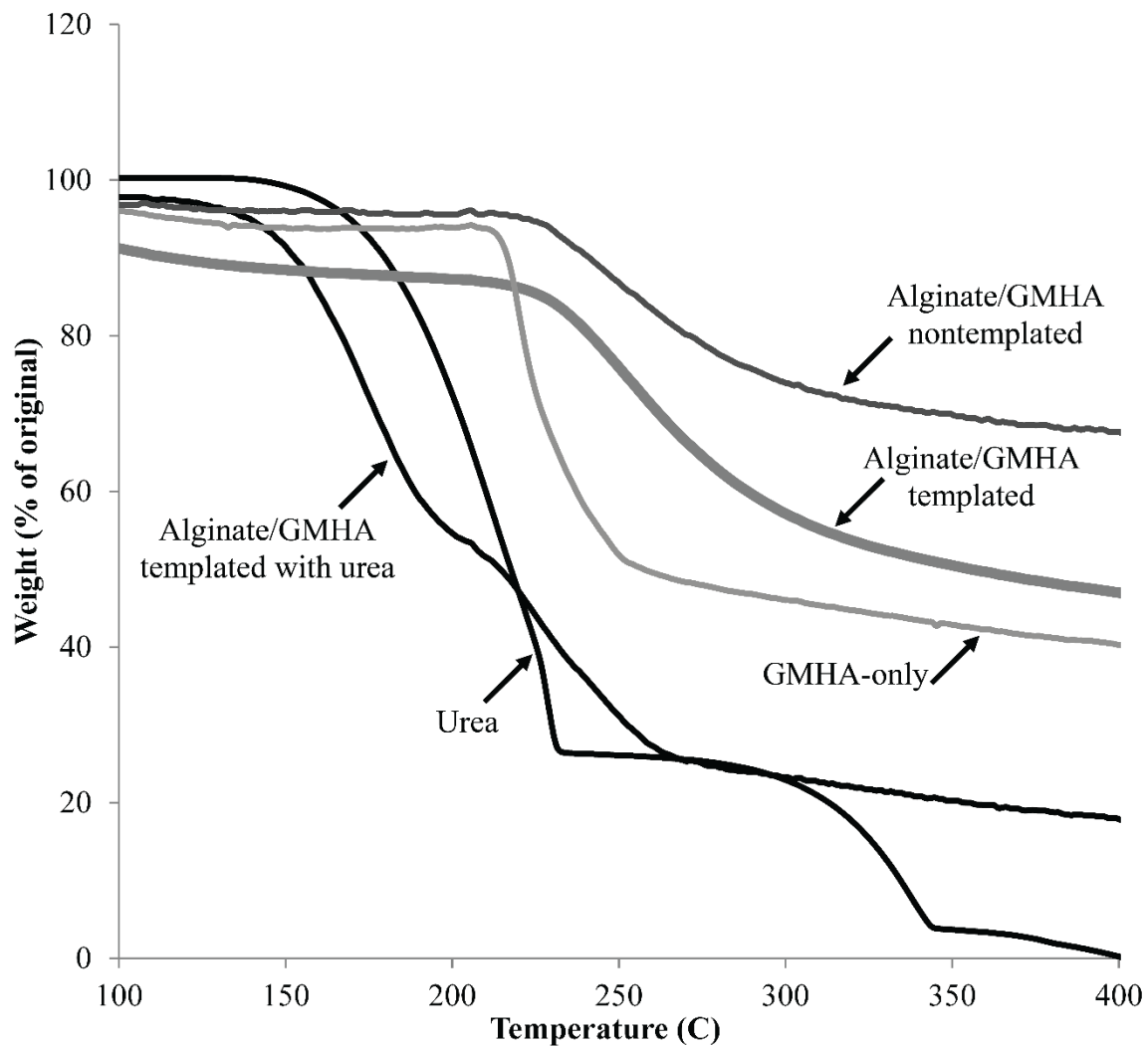
Figure S3. Thermogravimetric analysis (TGA) to confirm the complete removal of urea from the alginate/GMHA films after extensive washing.

$$Modulus \ (MPa) = \frac{Tensile \ strength \ (\frac{N}{mm^2})}{Elongation \ at \ break} \qquad [1]$$

$$E \ (\%) = 100\% \ * \ \frac{(L - L_0)}{L_0} \qquad [2]$$

$$TS \ \left(\frac{N}{mm2}\right) = \frac{F}{A} \qquad [3]$$

$$T = \int_0^{\varepsilon B} \sigma(d\varepsilon) \qquad [4]$$

Figure S4: Equations related to the mechanical properties of the films.
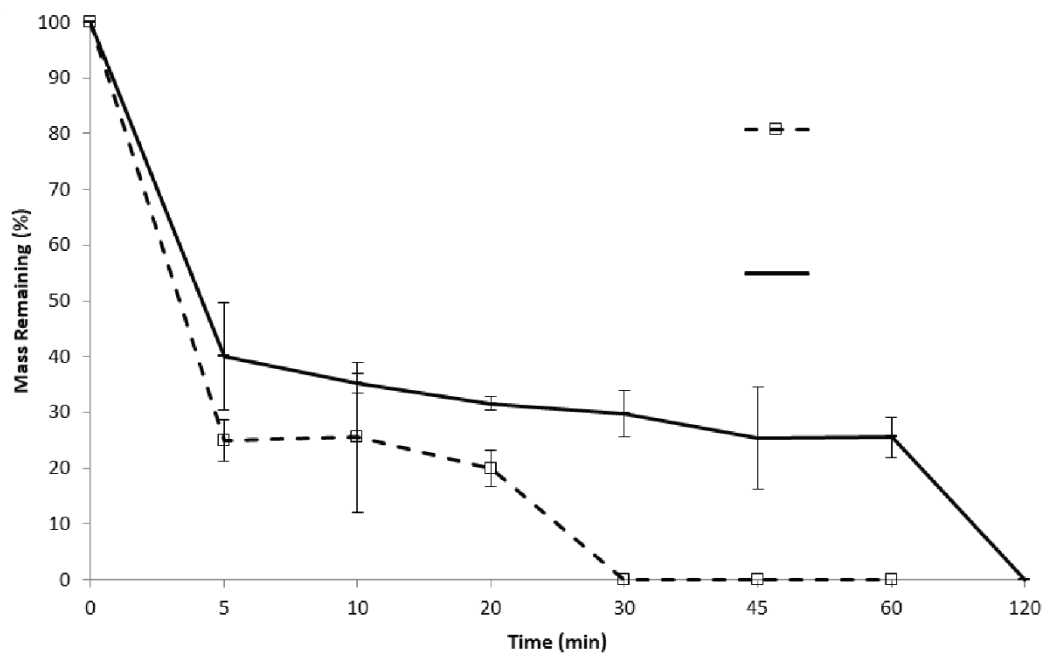
Figure S5: Dissolution of templated films compared to nontemplated films. Templated films degraded slower than nontemplated films. Nontemplated films went through complete dissolution with 30 min of exposure to 0.1 M citrate. An additional 90 min of exposure to 0.1 M citrate caused complete dissolution of the templated films. (N = 6).
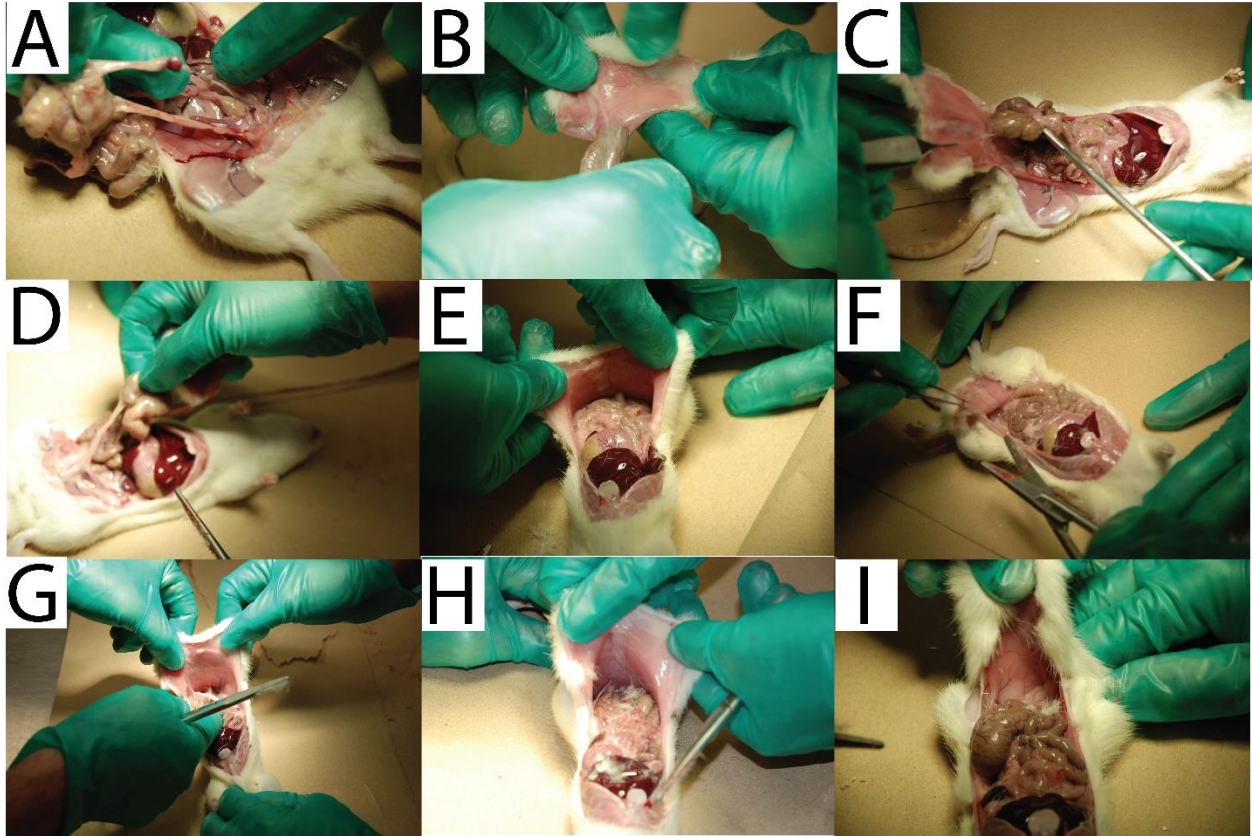
Figure S6: Examples of photographs of animals after surgery. *Control surgeries:* A) Rat 4529 – Grade 3. B) Rat 3557 – Grade 3. C) Rat 1525 – Grade 3. *Animals after implantation of Seprafilm®:* D) Rat 2455 – Grade 3. E) Rat 7443 – Grade 0. F) Rat 8451 – Grade 0. *Animals after implantation of alginate/GMHA films with sacrificial urea crystal template pores:* G) Rat 6715 – Grade 2. H) Rat 5717 – Grade 0. I) Rat 3734 – Grade 0.
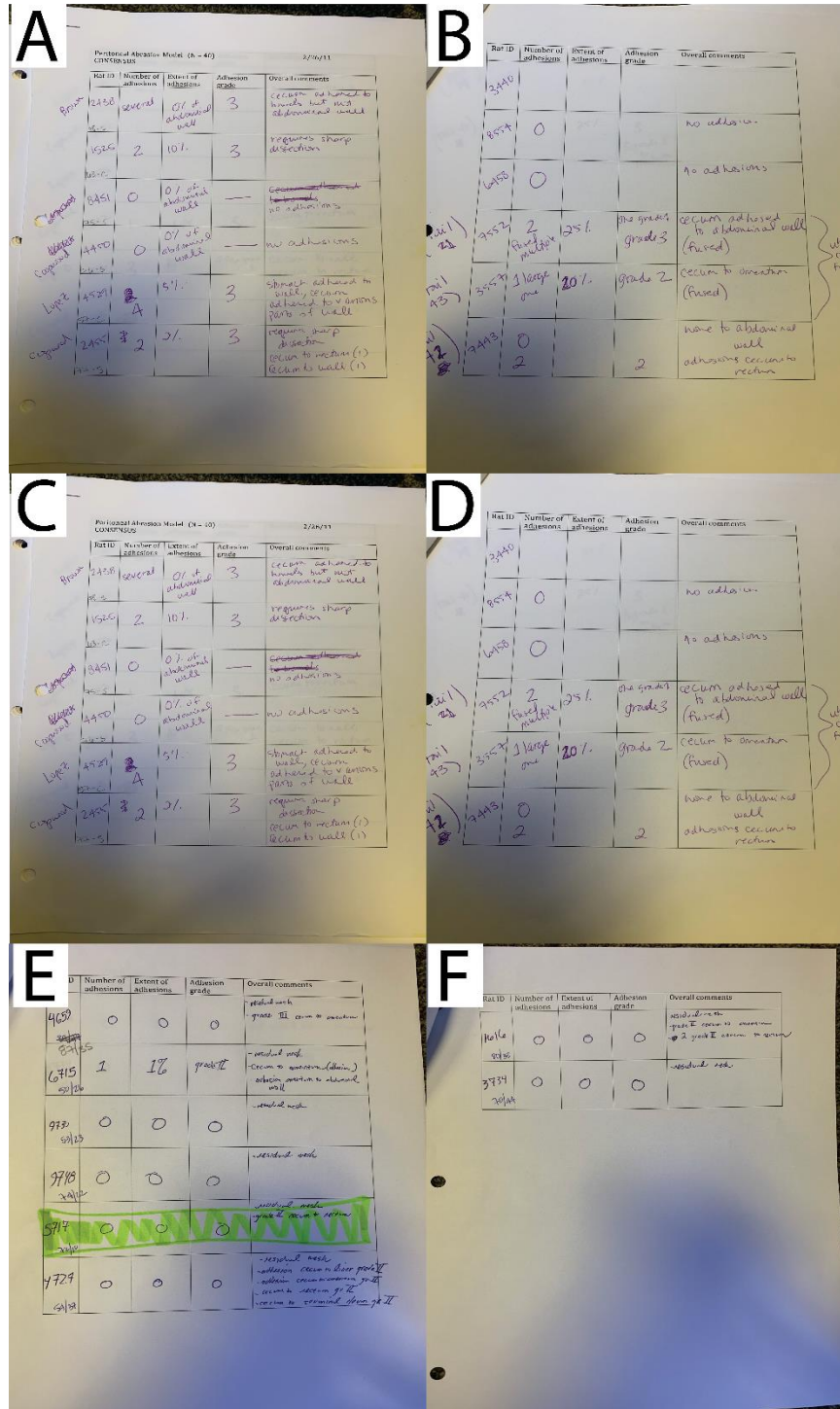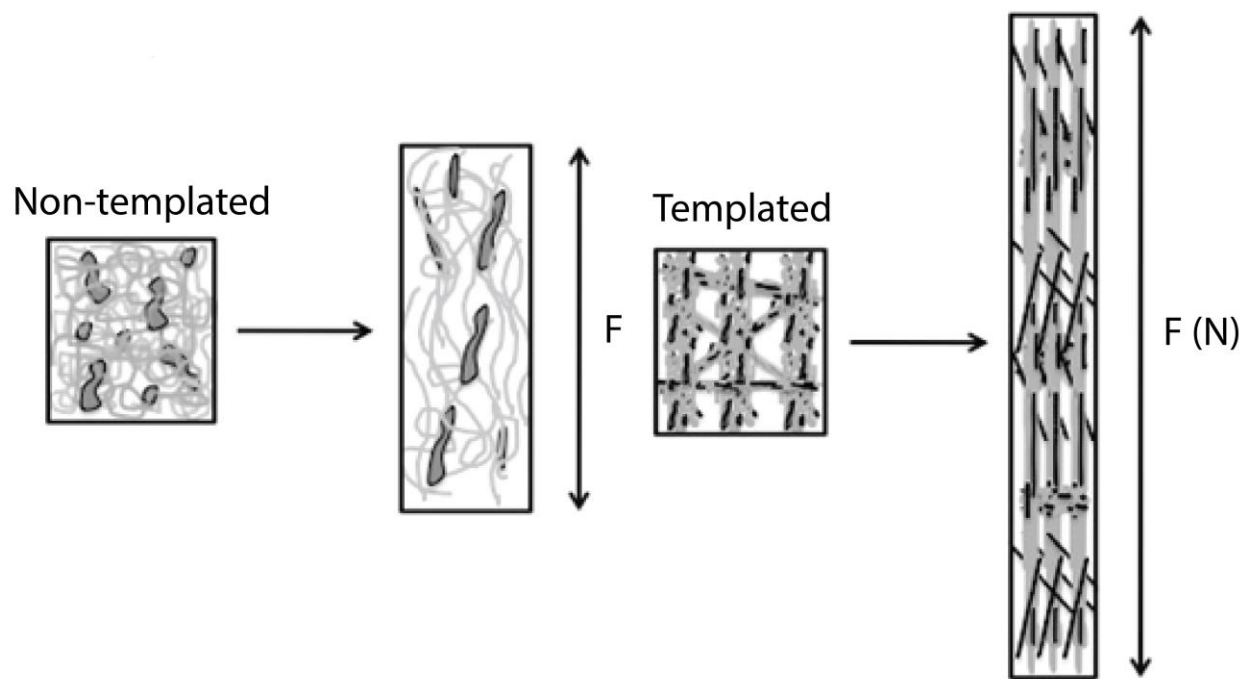
Figure S7: Examples of surgeon consensus sheets for animals after surgery. A&B) Control surgeries. C&D) Animals after implantation of Seprafilm®. E&F) Animals after implantation of alginate/GMHA films with sacrificial urea crystal template pores.

Scheme S1: Schematic illustrating the deformation of the films under tension.